CERN-TH/2002-237
IPPP/02/53
DCPT/02/106
September 2002

HERWIG: AN EVENT GENERATOR FOR e^+e^- LINEAR COLLIDERS

Stefano Moretti
CERN Theory Division, CH-1211 Geneva 23, Switzerland and
Institute for Particle Physics Phenomenology, Durham DH1 3LE, UK

I review all the new features of the HERWIG event generator which are relevant to Linear Collider (LC) physics starting from version 6.1.

1 Introduction

HERWIG is a general-purpose Monte Carlo (MC) event generator for high-energy processes [1], providing a full simulation of hard lepton-lepton, lepton-hadron and hadron-hadron scattering and soft hadron-hadron collisions in a single package, comprising the following features.
1. Initial- and final-state QCD jet evolution with soft gluon interference taken into account via angular ordering.
2. Colour coherence of (initial and final) partons in all subprocesses, including the production and decay of Supersymmetric (SUSY) particles.
3. Matrix Element (ME) corrections to the parton shower (PS) algorithm.
4. Spin correlations in the decay of heavy fermions.
5. Lepton beam polarisation in selected processes.
6. Azimuthal correlations within and between jets due to gluon interference and polarisation.
7. A cluster model for jet hadronisation (with optional colour rearrangement) based on non-perturbative gluon splitting and a similar model for soft and underlying hadronic events.
The HERWIG source codes and related information can be found in [2].

2 Linear Collider physics with HERWIG

Of particular relevance to the programme of future electron-positron LCs are items 3.–5. We will describe these in the following, after mentioning the Minimal Supersymmetric Standard Model (MSSM) processes currently available in lepton-antilepton annihilations.

2.1 MSSM processes in $\ell^+\ell^-$ collisions ($\ell = e, \mu$)

Starting from version 6.1, HERWIG includes the production and decay of (s)particles, as given by the MSSM. The conventions used and a detailed description of the implementation can be found in [3].

HERWIG does not contain any built-in models for SUSY-breaking scenarios. In all cases the general MSSM particle spectrum and decay tables must be provided just like those for any other object, with the following caveats: (i) SUSY particles do not radiate (which is reasonable if their decay lifetimes are much shorter than the QCD confinement scale); (ii) CP-violating SUSY phases are not included. A package, ISAWIG, has been created to work with ISAJET [4] to produce a file containing the SUSY particle masses, lifetimes, couplings and mixing parameters. This package takes the outputs of the ISAJET MSSM programs and produces a data file in a format that can be read into HERWIG for the subsequent process generation. The user can produce her/his own file provided that the correct format is used. To this end, we invite the consultation of the ISAWIG webpage [5], where some example of input files can be found (the SUSY benchmark points recommended in Ref. [6] are also available).

Table 1. The MSSM processes via $\ell^+\ell^-$ annihilations implemented in HERWIG.

IPROC	MSSM processes
700-99	R-parity conserving SUSY processes
700	$\ell^+\ell^- \to$ 2-sparticle processes (sum of 710–760)
710	$\ell^+\ell^- \to$ neutralino pairs (all neutralinos)
706+4IN1+IN2	$\ell^+\ell^- \to \widetilde{\chi}^0_{\rm IN1}\widetilde{\chi}^0_{\rm IN2}$ (IN1,2=neutralino mass eigenstate)
730	$\ell^+\ell^- \to$ chargino pairs (all charginos)
728+2IC1+IC2	$\ell^+\ell^- \to \widetilde{\chi}^+_{\rm IC1}\widetilde{\chi}^-_{\rm IC2}$ (IC1,2=chargino mass eigenstate)
740	$\ell^+\ell^- \to$ slepton pairs (all flavours)
736+5IL	$\ell^+\ell^- \to \widetilde{\ell}_{L,R}\widetilde{\ell}^*_{L,R}$ (IL $= 1,2,3$ for $\widetilde{\ell} = \tilde{e}, \tilde{\mu}, \tilde{\tau}$)
737+5IL	$\ell^+\ell^- \to \widetilde{\ell}_L\widetilde{\ell}^*_L$ (IL as above)
738+5IL	$\ell^+\ell^- \to \widetilde{\ell}_L\widetilde{\ell}^*_R$ (IL as above)
739+5IL	$\ell^+\ell^- \to \widetilde{\ell}_R\widetilde{\ell}^*_R$ (IL as above)
740+5IL	$\ell^+\ell^- \to \widetilde{\nu}_L\widetilde{\nu}^*_L$ (IL $= 1,2,3$ for $\widetilde{\nu}_e, \widetilde{\nu}_\mu, \widetilde{\nu}_\tau$)
760	$\ell^+\ell^- \to$ squark pairs (all flavours)
757+4IQ	$\ell^+\ell^- \to \widetilde{q}_{L,R}\widetilde{q}^*_{L,R}$ (IQ $= 1...6$ for $\widetilde{q} = \tilde{d}...\tilde{t}$)
758+4IQ	$\ell^+\ell^- \to \widetilde{q}_L\widetilde{q}^*_L$ (IQ as above)
759+4IQ	$\ell^+\ell^- \to \widetilde{q}_L\widetilde{q}^*_R$ (IQ as above)
760+4IQ	$\ell^+\ell^- \to \widetilde{q}_R\widetilde{q}^*_R$ (IQ as above)

In addition to the decay modes implemented in the ISAJET package, ISAWIG also includes the calculation of all 2-body squark/slepton and 3-body gaugino/gluino R-parity violating (RPV) decay modes (alas, RPV lepton-

gaugino and slepton-Higgs mixing is not considered). Moreover, the emulation of RPV processes is also a feature of the production stage. Tab. 1 illustrates all MSSM modes initiated by $\ell^+\ell^-$ scattering that are available at present (version 6.4). Here, `IPROC` is the input label selecting the hard process.

Table 1. Continues.

800-99	R-parity violating SUSY processes
800	Single sparticle production, sum of 810–840
810	$\ell^+\ell^- \to \widetilde{\chi}^0\nu_i$, (all neutralinos)
810+`IN`	$\ell^+\ell^- \to \widetilde{\chi}^0_{\rm IN}\nu_i$, (`IN`=neutralino mass state)
820	$\ell^+\ell^- \to \widetilde{\chi}^- e_i^+$ (all charginos)
820+`IC`	$\ell^+\ell^- \to \widetilde{\chi}^-_{\rm IC} e_i^+$, (`IC`=chargino mass state)
830	$\ell^+\ell^- \to \widetilde{\nu}_i Z^0$ and $\ell^+\ell^- \to \widetilde{\ell}_i^+ W^-$
840	$\ell^+\ell^- \to \widetilde{\nu}_i h^0/H^0/A^0$ and $\ell^+\ell^- \to \widetilde{\ell}_i^+ H^-$
850	$\ell^+\ell^- \to \widetilde{\nu}_i\gamma$
860	Sum of 870 and 880
870	$\ell^+\ell^- \to \ell^+\ell^-$, via LLE only
867+3`IL1`+`IL2`	$\ell^+\ell^- \to \ell^+_{\rm IL1}\ell^-_{\rm IL2}$ (`IL1,2`=1,2,3 for e,μ,τ)
880	$\ell^+\ell^- \to dd$, via LLE and LQD
877+3`IQ1`+`IQ2`	$\ell^+\ell^- \to d_{\rm IL1}\bar{d}_{\rm IL2}$ (`IQ1,2`=1,2,3 for d,s,b)

Table 1. Continues.

910-975	Higgs processes
910	$\ell^+\ell^- \to \nu_\ell\bar{\nu}_\ell h^0 + \ell^+\ell^- h^0$
920	$\ell^+\ell^- \to \nu_\ell\bar{\nu}_\ell H^0 + \ell^+\ell^- H^0$
960	$\ell^+\ell^- \to Z^0 h^0$
970	$\ell^+\ell^- \to Z^0 H^0$
955	$\ell^+\ell^- \to H^+H^-$
965	$\ell^+\ell^- \to A^0 h^0$
975	$\ell^+\ell^- \to A^0 H^0$

2.2 ME corrections to the standard PS

The study of top quark production and decay will be one of the main areas of research activity at future LCs. Hence, it is of paramount importance the availability of a MC event generator describing the dynamics of the $e^+e^- \to t\bar{t} \to b\bar{b}W^+W^-$ process ($m_t = 175$ GeV) with great accuracy. As the top quark is a coloured particle, of particular concern are higher order effects from QCD. Whereas those induced by the exchange of virtual gluons do not change the lowest order kinematics, real radiation of the latter does so. This is of relevance when it comes to reconstruct the top quark parameters (primarily, m_t and Γ_t) from some exclusive jet observables, in presence of $W^\pm \to$ jet-jet decays.

According to the HERWIG standard algorithm for PS, gluon radiation is

treated in the soft and collinear approximation and no emission is permitted in the 'dead zones' (hard and large-angle parton radiation) seen in the left-hand side of Figs. 1–2. The current version of the HERWIG event generator has been improved by applying so-called ME corrections: i.e., the dead zone is populated by the use of the exact first-order matrix element ('hard correction') and the $\mathcal{O}(\alpha_S)$ result is used in the already-filled region any time an emission is the 'hardest so far' ('soft correction') [7].

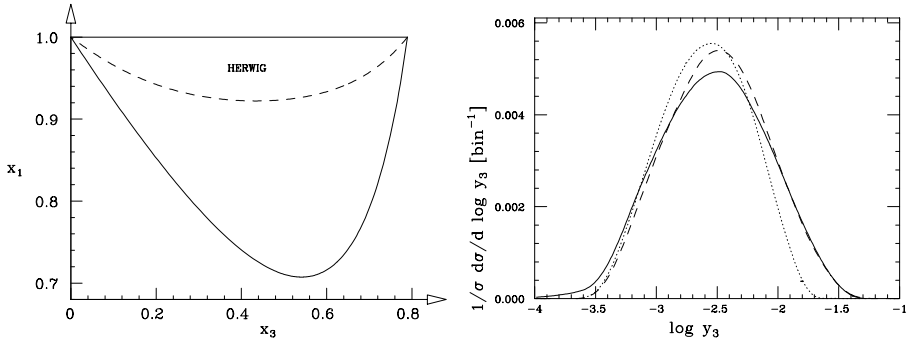

Figure 1: The $t \to W_1^+ b_2 g_3$ decay: (Left) The total (solid) and HERWIG (dashed) phase space in terms of the x_1 and x_3 momentum fractions; (Right) The y_3 distributions according to the new HERWIG implementation (dashed), to the old one (dotted) and to the exact $\mathcal{O}(\alpha_S)$ calculation (solid). Rates are at 360 GeV.

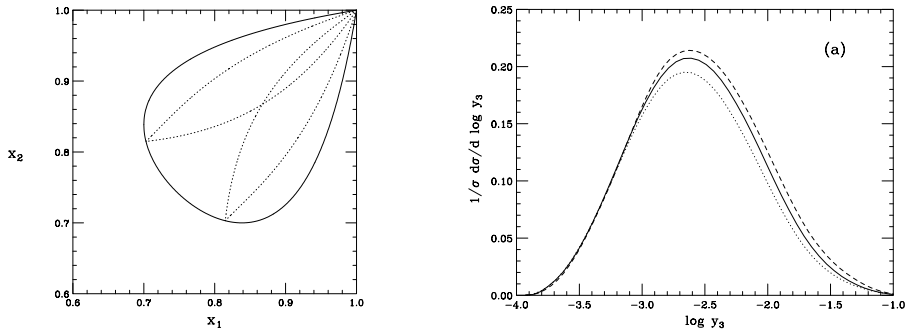

Figure 2: The $e^+e^- \to t_1\bar{t}_2 g_3$ production: (Left) Total (solid) and HERWIG (dotted) phase space limits for $t\bar{t}$ production in terms of the x_1 and x_3 momentum fractions; (Right) The y_3 distributions according to the old HERWIG implementation (dashed), to the new one, the latter populating either the small- and large-angle (solid) or only the large-angle region (dotted) of the dead zone. Rates are at 500 GeV.

A good measure to gauge the improvement due to the new algorithm can be gained from investigating the threshold value of the Durham jet-clustering algorithm [8] for all events to yield three jets, each with $E_T > 10$ GeV and relative $\Delta R > 0.7$ in transverse energy and cone separation. Just above $\sqrt{s} = 2m_t$, where real radiation from the production stage is negligible, the beneficial effects of the new HERWIG implementation can be appreciated in the right-hand side of Fig. 1, in the case of top quark decays. At large y_3 values, where the fixed order $\mathcal{O}(\alpha_S)$ description [9] is expected to well describe the underlying (hard gluon) dynamics, we see the latter to coincide with the current HERWIG description, which in turns retains sizable differences from the $\mathcal{O}(\alpha_S)$ result as $y_3 \to 0$ (soft and collinear gluon), where the all-order PS algorithm is known to be reliable. While similar improvements can be seen in the case of top quark production, it is in this instance more instructive to compare the same y_3 distribution as obtained from the old HERWIG description (incorporating ME corrections but not the complete $\sim m_t^2/s$ mass effects) to those given by two more advanced options, currently being implemented: the default one filling both the small- and large-angle dead zones and the intermediate one occupying only the large-angle region, both accounting for the above mass corrections (see the right-hand side of Fig. 2). The sizable differences between the three clearly makes the point in favour of the more complete HERWIG implementation in view of future LC studies.

Another example of ME corrections available in HERWIG is the case of multi-jet production in electron-positron annihilations via exact fixed-order $e^+e^- \to n$ parton MEs, limitedly to the case $n = 4$. Here, the event generation can be initiated by the $e^+e^- \to q\bar{q}gg$ and $e^+e^- \to q\bar{q}Q\bar{Q}$ MEs, with the four parton 'interfaced' to the subsequent PS [10] (i.e., a hard cut-off is enforced in order to separate the partons thus preventing the MEs from diverging and the PS is attached to each of the latter only over the reduced phase space). This is an alternative to the standard description based on the $e^+e^- \to q\bar{q}(g)$ hard scattering process followed by the traditional PS algorithm. While the new implementation is only reliable for $n \geq 4$ and for jet separations larger than the corresponding partonic cut-off, it remedies the drawback of the old one in describing the angular orientation of four-jet events, as seen by, e.g., the ALEPH Collaboration [11] (see also Ref. [12]).

The ability of a MC event generator to describe correctly a four-jet final state is particularly relevant in the context of LC searches for a light Higgs state, predominantly produced via $e^+e^- \to ZH \to 4$ jets events, as BR[$Z \to$ jet-jet]=0.7 and BR[$H \to b\bar{b}$] ≈ 1. Take for example an hadronic sample composed of two b-jets and two untagged jets at a 500 GeV LC, selected by using the Durham jet-clustering algorithm with resolution $y_4 = 0.001$ and with

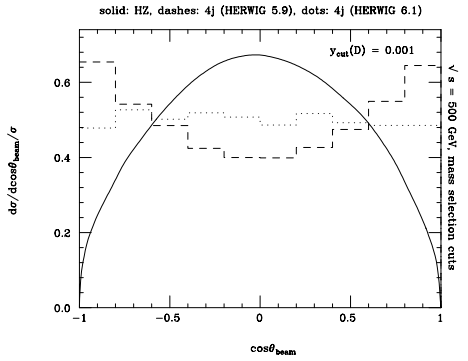

Figure 3: Distributions for the polar angle of the reconstructed Z for the Higgs signal and the two description of the QCD four-jet background mentioned in the text.

one pair of jets reproducing the Z mass within 10 GeV, i.e. $|M_{\rm jj} - M_Z| < 10$ GeV. Then compare the polar angle distribution of the di-jet system emulating a Z decay, for the QCD four-jet background and the above Higgs signal (for $M_H = 150$ GeV): see Fig. 3. It is clear that, in the region populated by the latter, the discrepancy between the old (HERWIG v5.9) and new (HERWIG v6.1) description of the former is rather large, similar in size to the signal excess. Needless to say, under these circumstances, a clear understanding of the behaviour of the QCD background is crucial in order to extract the Higgs resonance and measure its relevant parameters (M_H, Γ_H, etc.) [a].

A more sophisticated implementation 'matching' MEs and PS, meaning the procedure of exploiting a combined approach which uses MEs for large phase space separations, PS in the infrared (i.e., soft and collinear) limit and modified (by Sudakov form factors) MEs in the overlapping region [15], is available in APACIC++, for $n \leq 6$ [16] [b].

2.3 Spin correlations and lepton beam polarisation

Since v6.4, spin correlations are available in processes where SUSY particles, top quarks and τ-leptons are produced [18]. Whenever these particles decay, 2-, 3- and 4-body MEs are used to describe their dynamics (with or without the spin correlations). In the case of τ's, an interface to TAUOLA [19] is also available. Polarisation has been implemented for incoming leptonic beams in

[a] Options similar to the one available in HERWIG for $n = 4$ can also be found in PYTHIA [13] and 4JPHACT [14].

[b] A similar standalone implementation for $n \leq 4$ is available in HERWIG too [17].

SUSY processes. These effects are included both in the production of SUSY particles and via the spin correlation algorithm in their decays.

As an example of the impact of such spin effects, consider pair production of the two lightest neutralinos at an (un)polarised LC, via the following graphs:

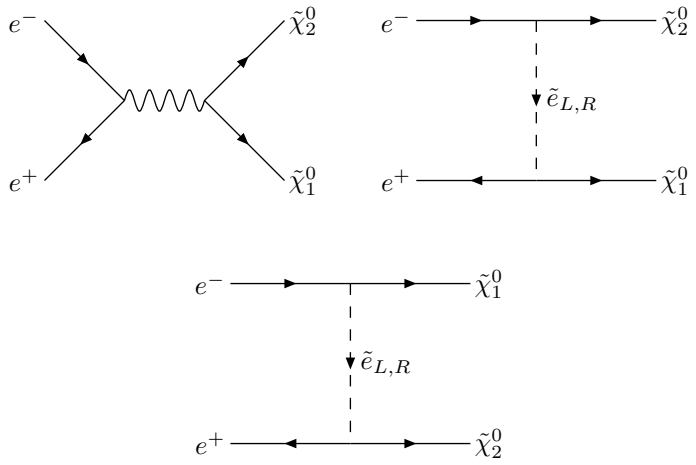

with $\tilde{\chi}_1^0$ the Lightest Supersymmetric Particle (LSP) and $\tilde{\chi}_2^0$ decaying via:

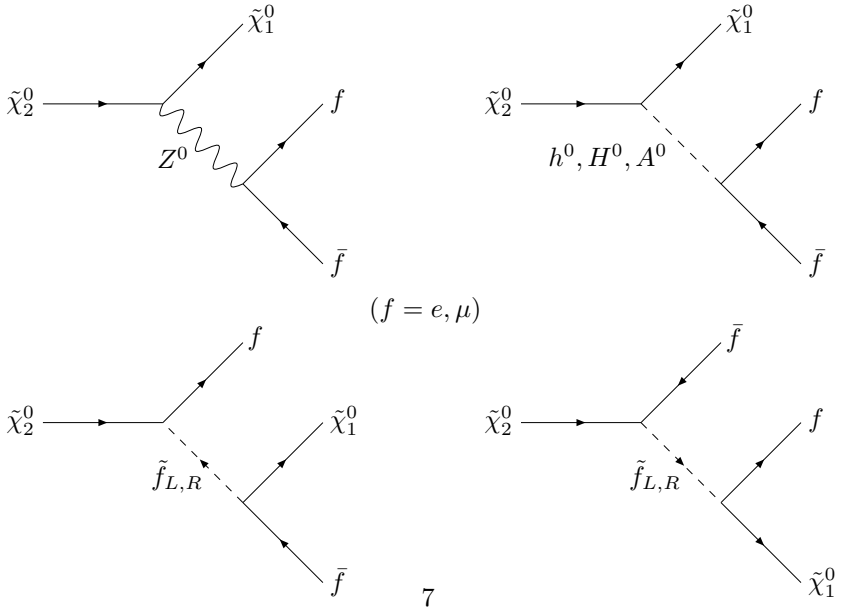

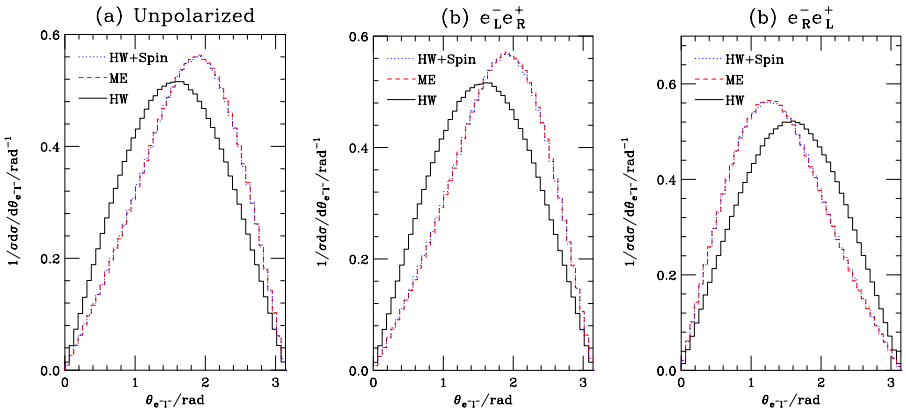

Figure 4: Angle between the lepton produced in $e^+e^- \to \tilde{\chi}^0_2\tilde{\chi}^0_1 \to f\bar{f}\tilde{\chi}^0_1\tilde{\chi}^0_1$ ($f = e, \mu$) and the incoming electron beam in the laboratory frame for $\sqrt{s} = 500$ GeV with: (a) no polarization, (b) negatively polarized electrons and positively polarized positrons and (c) positively polarized electrons and negatively polarized positrons. The solid line shows the default result from HERWIG which treats the production and decay as independent, the dashed line gives the full result from the four-body ME and the dotted line the result of the spin correlation algorithm. (The SUSY parameters are: $M_0 = 210$ GeV, $A_0 = 0$, $\tan\beta = 10$, $M_1 = 450$ GeV, $M_{2,3} = 350$ GeV.)

From Ref. [18], we show Fig. 4, illustrating the angular behaviour of the above SUSY signals, as given by a typical MC implementation (`HW`), which does not include spin effects in production and decay and/or ME corrections in the latter, to the output of HERWIG v6.4 (`HW+Spin`). Once again, the improvement is clear if one confronts the latter with the distributions obtained from a complete calculation (`ME`), wherein the event generation is based on the exact $2 \to 6$ ME description.

I thank the LCWS2002 organisers for the excellent atmosphere and stimulating environment that they have created during the workshop and The Royal Society of London, UK, for partial financial support in the form of a Conference Grant.

1. G. Marchesini, B.R. Webber, G. Abbiendi, I.G. Knowles, M.H. Seymour and L. Stanco, *Comput. Phys. Commun.* **67**, 465 (1992); G. Corcella, I.G. Knowles, G. Marchesini, S. Moretti, K. Odagiri, P. Richardson, M.H. Seymour and B.R. Webber, `hep-ph/9912396`; *JHEP* **01**, 010 (2001); `hep-ph/0107071`; `hep-ph/0201201`.

2. See: http://hepwww.rl.ac.uk/theory/seymour/herwig/.
3. S. Moretti, K. Odagiri, P. Richardson, M.H. Seymour and B.R. Webber, *JHEP* **04**, 028 (2002); S. Moretti, hep-ph/0205105.
4. F.E. Paige, S.D. Protopopescu, H. Baer and X. Tata, hep-ph/9804321; hep-ph/ 9810440.
5. See: http://www.hep.phy.cam.ac.uk/~richardn/HERWIG/ISAWIG/.
6. B.C. Allanach *et al.*, *Eur. Phys. J.* C **25**, 113 (2002).
7. G. Corcella and M.H. Seymour, *Phys. Lett.* B **442**, 417 (1998); hep-ph /9911335; G. Corcella, E.K. Irish and M.H. Seymour, hep-ph/0012319.
8. Yu.L. Dokshitzer, contribution cited in the 'Report of the Hard QCD Working Group', in Proceedings of the Workshop 'Jet Studies at LEP and HERA', Durham, December 1990, *J. Phys* G **17**, 1537 (1991); S. Catani, Yu.L. Dokshitzer, M. Olsson, G. Turnock and B.R. Webber, *Phys. Lett.* B **269**, 432 (1991).
9. L.H. Orr, T. Stelzer and W.J. Stirling, *Phys. Lett.* B **354**, 442 (1995); *Phys. Rev.* D **56**, 446 (1997).
10. S. Moretti, hep-ph/000819.
11. ALEPH Collaboration, *Z. Phys.* C **76**, 1 (1997).
12. A. Ballestrero *et al.*, *J. Phys.* G **24**, 365 (1998); S. Moretti and W.J. Stirling, *Eur. Phys. J.* C **9**, 81 (1999).
13. T. Sjöstrand, L. Lönnblad and S. Mrenna, hep-ph/0108264.
14. A. Ballestrero, in preparation.
15. S. Catani, F. Krauss, R. Kuhn and B.R. Webber, *JHEP* **11**, 063 (2001).
16. F. Krauss, R. Kuhn and G. Soff, *J. Phys.* G **26**, L11 (2000); *Acta Phys. Polon.* B **30**, 3875 (1999).
17. See: http://webber.home.cern.ch/webber/.
18. P. Richardson, *JHEP* **11**, 029 (2001).
19. S. Jadach, Z. Was, R. Decker and J.H. Kuhn, Comput. *Phys. Commun.* **76**, 361 (1993); M. Jezabek, Z. Was, S. Jadach and J.H. Kuhn, Comput. *Phys. Commun.* **70**, 69 (1992); S. Jadach, J.H. Kuhn and Z. Was, Comput. *Phys. Commun.* **64**, 275 (1990).